system can "freeze in" the pattern as the result of developmentally determined changes in its chemical environment.

REFERENCES AND NOTES

1. A. M. Turing, *Philos. Trans. R. Soc. London Ser. B* **237**, 37 (1952).
2. H. Meinhardt, *Models of Biological Pattern Formation* (Academic Press, London, 1982).
3. J. D. Murray, *Mathematical Biology* (Springer-Verlag, Berlin, 1989).
4. T. Nozakura and S. Ikeuchi, *Astrophys. J.* **279**, 40 (1984).
5. M. Maruyama, *Am. Sci.* **51**, 164 (1963).
6. V. Castets, E. Dulos, J. Boissonade, P. De Kepper, *Phys. Rev. Lett.* **64**, 2953 (1990).
7. P. De Kepper, V. Castets, E. Dulos, J. Boissonade, *Physica D* **49**, 161 (1991).
8. Q. Ouyang and H. L. Swinney, *Nature* **352**, 610 (1991).
9. I. Lengyel, Gy. Rábai, I. R. Epstein, *J. Am. Chem. Soc.* **112**, 4606 (1990); *ibid.*, p. 9104.
10. I. R. Epstein, I. Lengyel, S. Kádár, M. Yokoyama, M. Kagan, *Physica A* **188**, 26 (1992).
11. I. Lengyel, S. Kádár, I. R. Epstein, *Phys. Rev. Lett.* **69**, 2729 (1992).
12. A homogeneous steady state is stable to homogeneous perturbation if $K' > H_1$ and can be destabilized by diffusion if $H_1 > H_2 > 0$. Here

$$H_1 = -\frac{a_{11}}{a_{22}} - 1$$

$$H_2 = \frac{-a_{11}}{2\sqrt{c(a_{11}a_{22} - a_{12}a_{21})} - ca_{11}} - 1$$

where a_{ij} are the elements of the Jacobian matrix of the complex-free system and K' is the stability constant of the complex that binds the activator species.
13. K. Agladze, E. Dulos, P. De Kepper, *J. Phys. Chem.* **96**, 2400 (1992).
14. I. Lengyel and I. R. Epstein, *Proc. Natl. Acad. Sci. U.S.A.* **89**, 3977 (1992).
15. ———, *Science* **251**, 650 (1991).
16. W. H. Press, B. P. Flannery, S. A. Teukolsky, W. T. Vetterling, *Numerical Recipes* (Cambridge Univ. Press, Cambridge, 1989).
17. S. A. Newman and W. D. Comper, *Development* **110**, 1 (1990).
18. The possibility of obtaining batch Turing structures was first suggested to us by A. Winfree. We thank K. Kustin for helpful suggestions. This work was supported by the National Science Foundation (CHE-9023294) and by a U.S.–Hungarian grant from the National Science Foundation and the Hungarian Academy of Sciences.

4 September 1992; accepted 20 November 1992

A Cationic Cesium Continuum in Zeolite X

Tao Sun, Karl Seff,* Nam Ho Heo, Vitalii P. Petranovskii

A cesium continuum that fills the channels and cavities of zeolite X has been prepared, and its structure has been determined by single-crystal x-ray crystallography. The three-dimensional continuum is cationic to balance the negative charge of the zeolite framework. Its valence electrons, only 0.3 per Cs^+ ion, are widely delocalized over 95 percent of the cesium ions in the crystal. The continuum has a unit cell formula of $(Cs_{122})^{86+}$ and contains Cs_{13} and Cs_{14} clusters (one per supercage) arranged like the atoms in diamond, with one Cs_2 appendix (in the sodalite cavity) per cluster.

Zeolites with guest species incorporated in their nanometer-dimension windows, channels, and cavities can have novel optical and electronic properties (*1*, *2*). An interesting subclass of such materials could be produced by filling zeolites with metals. If the guest metal were the same element as the extraframework cations already present in the zeolite, it might be stabilized within the zeolite by electron delocalization. The result would be an arrangement of metal atoms, different from that of the metal itself, containing far less than a stoichiometric number of electrons.

Zeolite X (*3*) (of idealized composition $NaSiAlO_4$) has an aluminosilicate framework that may be viewed as an assemblage of sodalite cavities, cubo-octahedra of composition $(Si_{12}Al_{12}O_{48})^{12-}$ (Fig. 1A), which are arranged in space (Fig. 1B) like the carbon atoms in diamond. They are joined at alternating 6-oxygen rings by six bridging oxygen atoms, not shown in Fig. 1A, one bound to each vertex of Fig. 1A to complete a tetrahedron. This leads to the existence of small double 6-ring cavities and large supercages (Fig. 1B). The extraframework cations that compensate for the negative charge of the framework occupy the various positions indicated in Fig. 1B by Roman numerals.

Earlier work has shown that zeolites exposed to alkali metal vapor can absorb extra alkali metal atoms into their cavities to form clusters. By using the electron spin resonance (ESR) technique, Kasai and Rabo (*4–7*), Edwards *et al.* (*8–11*), Martens *et al.* (*12–14*), Xu and Kevan (*15*, *16*), and Smeulders *et al.* (*17*, *18*) were able to detect paramagnetic clusters in zeolites A, X, and Y and sodalite. The cationic clusters Na_6^{5+}, Na_5^{4+}, Na_4^{3+}, K_4^{3+}, and K_3^{2+} were found in sodalite cavities. Metallic particles were also found in the supercages of zeolites X and Y, but the ESR method is ineffective at describing them. In general, no attempt was made to control stoichiometry or to achieve high loadings. Recently, K_{n+4}^{n+} was reported in zeolite A (*19*).

We studied the products of the reactions of zeolite A with Cs and Rb vapor by single-crystal x-ray diffraction (*20–26*). The triangular cluster Rb_3^{n+} [n = 1 (*20*) or 2 (*21*)], synthesized by exposing dehydrated zeolite A to Rb vapor, was found crystallographically in the sodalite unit of zeolite A; Rb_3^{n+} is stabilized by coordination to between one and three Rb^+ cations. The linear Cs_4^{3+} cluster, which extends from a large cavity through a sodalite unit into another large cavity, was found in zeolite A (*22–26*).

This study was initiated with the hope that fully Cs^+-exchanged zeolite X could be prepared from Na–zeolite X (Na-X) by redox reaction with Cs gas, as had been done with zeolite A (*22–26*). Full exchange of Cs for Na has not been achievable by conventional aqueous methods of ion exchange (*27–29*). In addition, it was hoped that excess Cs atoms would be sorbed to form Cs clusters, as had occurred in zeolite A (*22–26*).

Large single crystals of Na-X with the stoichiometry $Na_{92}Al_{92}Si_{100}O_{384}$ were prepared in St. Petersburg, Russia (*30*). One of these, a colorless octahedron ~0.25 mm on an edge, was lodged in a

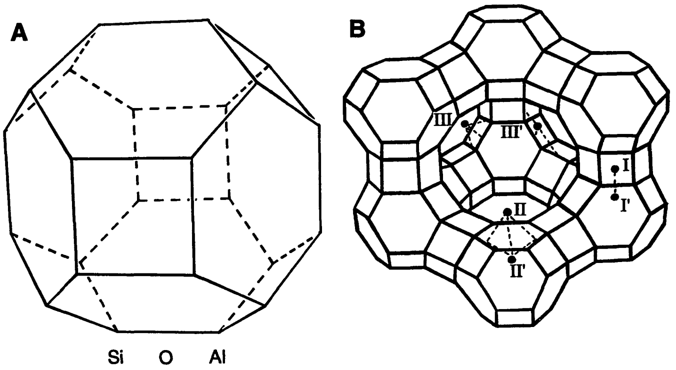

Fig. 1. Framework structures of a sodalite cavity (**A**) and of zeolite X (**B**). Extraframework cation positions are labeled with Roman numerals.

T. Sun and K. Seff, Department of Chemistry, University of Hawaii, Honolulu, HI 96822.
N. H. Heo, Department of Industrial Chemistry, Kyungpook National University, Taegu 702-701, South Korea.
V. P. Petranovskii, A. F. Ioffe Physical Technical Institute, Academy of Sciences of Russia, St. Petersburg 194021, Russia.

*To whom correspondence should be addressed.

quartz capillary tube that was connected to a vacuum line. After complete dehydration at 450°C and 10^{-6} torr, the crystal was exposed to Cs vapor at 450°C. The black lustrous product was sealed off under vacuum after cooling to room temperature.

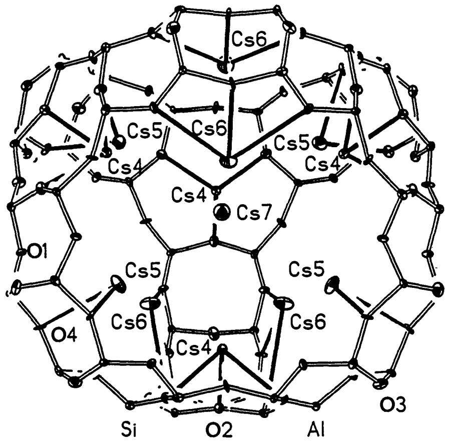

Fig. 2. The arrangement of Cs atoms that minimizes repulsive interactions in 75% of the supercages in Cs–zeolite X. (Each of the remaining supercages contains an additional Cs atom.) Ellipsoids of 20% probability are shown.

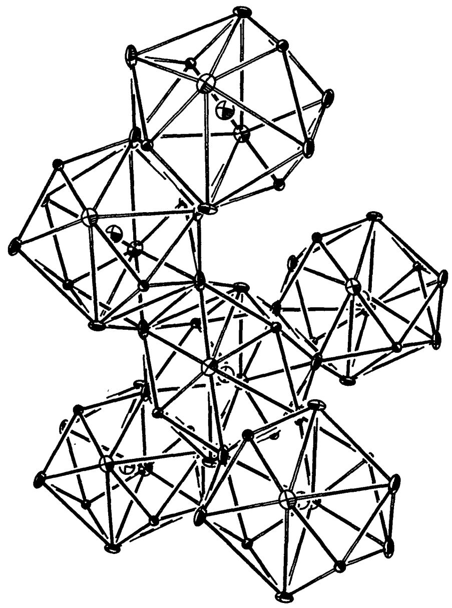

Fig. 3. A portion of the Cs continuum formed in the supercage cavities of Cs–zeolite X. The central icosahedral unit shows its full tetrahedral bonding to four other units. The distances from the Cs atoms at the center of an icosahedral cluster to surrounding partially reduced Cs^+ ions range from 5.00 to 5.40 Å. Distances among these surrounding ions range from 4.66 to 7.27 Å, with more than half at distances less than 5.00 Å, ensuring full continuity within the icosahedral cluster. Distances connecting icosahedra range from 4.84 to 4.97 Å. Ellipsoids of 20% probability are shown.

The crystal structure was solved in the space group $Fd\bar{3}$. The error index decreased from R = 0.15 to its final value, 0.062, when the Cs7 atoms were included at the centers of the supercages. The crystallographic result indicates a composition of $Cs_{128}Al_{92}Si_{100}O_{384}$ per 25.155 Å cubic unit cell. A Cs cluster develops in every sodalite and supercage cavity, and these clusters are bound together to form a single macroscopic cluster of the size of the single crystal. A Cs found at the very center of each supercage (Fig. 2) is not close to any framework oxide and is believed to be a near-neutral Cs atom. Surrounding it and in contact with the zeolite framework, 12 Cs^+ ions form a slightly distorted icosahedron (Fig. 2). Each such body-centered icosahedral cluster is in contact with four other similar clusters arranged tetrahedrally in adjacent supercages to form a continuum (Fig. 3). In each sodalite cavity, there is a partially reduced Cs_2 group that joins the continuum through a Cs of an icosahedral cluster to form (locally) a linear Cs_3 subcluster (Fig. 4). Partial reduction can be seen in the Cs–Cs bond distances of the subcluster, 3.89 ± 0.02 and 3.92 ± 0.02 Å, which are too short for unmoderated Cs^+–Cs^+ contacts.

Altogether, 128 Cs atoms are found per unit cell in this structure, many more than the 92 Cs^+ ions required to balance the negative charge of the zeolite framework. This result indicates that 36 Cs atoms per unit cell were sorbed into zeolite cavities. The ions at the centers of double 6-rings are octahedrally coordinated by framework O atoms and are not close to other Cs atoms, so they may be considered to be simple (not partially reduced) Cs^+ cations. Therefore, because each unit cell contains eight sodalite and eight supercage cavities, there are 36/8 = 4.5 electrons, more or less delocalized, in each sodalite-supercage pair of cavities. One of these electrons should reside principally on the Cs at the icosahedral cluster center and another may be relatively localized within each Cs_3 subcluster, but the remainder may be widely delocalized as in a metal over the icosahedral cluster continuum.

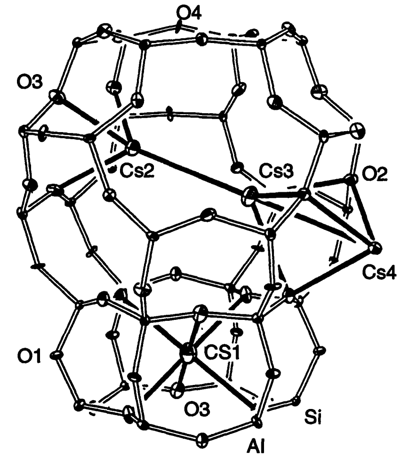

Fig. 4. A linear tricesium subcluster that fills a sodalite cavity and extends into a supercage, and a Cs^+ ion in a double 6-ring cavity. Bold lines indicate bonds from Cs atoms to O atoms of the zeolite framework and to each other. Ellipsoids of 20% probability are shown.

The Cs occupancies indicate that not all sodalite and supercage cavities have this ideal arrangement, partly because the Si/Al ratio is not 1.00. About 25% of the icosahedra are expanded by an additional Cs atom.

Compared to zeolite A, which can only accept 0.5 to 1.0 Cs atom per 12 Cs^+ ions per unit cell [(0.5 to 1.0)/12 ≤ 0.083], zeolite X of the composition studied has a much greater capacity for Cs atoms (36/92 = 0.39), perhaps because the supercage of zeolite X can accommodate a large cluster with an atom at its center.

Our results indicate that all sodalite and supercage cavities are "full" of Cs atoms and ions in this structure. Each sodalite cavity contains two Cs ions (at sites I′ and II′, Fig. 1B), which attach to the continuum by way of a large-cavity Cs at site II. Sites I′, II′, and II are colinear. Most Cs atoms and ions participate in a cationic continuum with a unit cell formula of $(Cs_{122})^{86+}$. Six additional Cs^+ ions are found at the centers of double 6-rings (site I). The continuum, per unit cell, consists of eight prismatic clusters, six of which are body-centered icosahedra (13 Cs atoms) (sites II, III, III′, and the center of the supercage) and two of which are expanded to contain an additional Cs atom. These clusters, arranged like the carbon atoms in diamond, are tetrahedrally connected to give the continuum (Fig. 3). The aluminosilicate zeolite framework (Fig. 1B) and the cesium continuum (Fig. 3) are interpenetrating, tetrahedrally connected continua of approximately equal volume.

REFERENCES

1. G. A. Ozin, A. Kuperman, A. Stein, *Angew. Chem. Int. Ed. Engl.* **28**, 359 (1989).
2. G. D. Stucky and J. E. Mac Dougall, *Science* **247**, 669 (1990).
3. D. W. Breck, *Zeolite Molecular Sieves* (Wiley, New York, 1974), pp 92–107.
4. P. H. Kasai, *J. Chem. Phys.* **43**, 3322 (1965).
5. J. A. Rabo, C. L. Angell, P. H. Kasai, V. Schomaker, *Discuss. Faraday Soc.* **41**, 328 (1966).
6. J. A. Rabo and P. H. Kasai, *Prog. Solid State Chem.* **9**, 1 (1976).
7. P. H. Kasai and R. J. Bishop, Jr., *ACS Monogr.* **171**, 350 (1976).
8. P. P. Edwards *et al.*, *J. Chem. Soc. Chem. Commun.* **1984**, 982 (1984).
9. M. R. Harrison *et al.*, *J. Solid State Chem.* **54**, 330 (1984).
10. P. A. Anderson, R. J. Singer, P. P. Edwards, *J. Chem. Soc. Chem. Commun.* **1991**, 914 (1991).
11. P. A. Anderson and P. P. Edwards, *ibid.*, p. 915.
12. L. R. M. Martens, P. J. Grobet, P. A. Jacobs, *Nature* **315**, 568 (1985).

13. L. R. M. Martens, P. J. Grobet, W. J. M. Vermeiren, P. A. Jacobs, in *New Developments in Zeolite Science and Technology*, A. Murakami, A. Iijima, J. W. Ward, Eds. (Kodansha, New York, 1986), pp. 935–941.
14. L. R. M. Martens, W. J. M. Vermeiren, P. J. Grobet, P. A. Jacobs, *Stud. Surf. Sci. Catal.* **31**, 531 (1987).
15. B. Xu and L. Kevan, *J. Chem. Soc. Faraday Trans.* **87**, 2843 (1991).
16. ______, *J. Phys. Chem.* **96**, 2642 (1992).
17. J. B. A. F. Smeulders *et al.*, *Zeolites* **7**, 347 (1987).
18. R. E. Breuer, E. deBoer, G. Geismar, *ibid.* **9**, 336 (1989).
19. Y. Nozue, T. Kodaira, T. Goto, *Phys. Rev. Lett.* **68**, 3789 (1992).
20. S. H. Song, Y. Kim, K. Seff, *J. Phys. Chem.* **95**, 9919 (1991).
21. S. H. Song, U. S. Kim, Y. Kim, K. Seff, *ibid.*, in press.
22. N. H. Heo and K. Seff, *J. Am. Chem. Soc.* **109**, 7986 (1987).
23. ______, *J. Chem. Soc. Chem. Commun.* **1987**, 1225 (1987).
24. N. H. Heo, C. Dejsupa, K. Seff, *J. Phys. Chem.* **91**, 3943 (1987).
25. C. Dejsupa, N. H. Heo, K. Seff, *Zeolites* **9**, 146 (1989).
26. N. H. Heo and K. Seff, *ibid.* **12**, 819 (1992).
27. R. M. Barrer, L. V. C. Rees, M. J. Shamsuzzoha, *J. Inorg. Nucl. Chem.* **30**, 333 (1968).
28. H. S. Sherry, *J. Phys. Chem.* **70**, 1158 (1966).
29. B. K. G. Theng, E. Vansant, J. B. Uytterhoeven, *Trans. Faraday Soc.* **64**, 3370 (1968).
30. V. N. Bogomolov and V. P. Petranovskii, *Zeolites* **6**, 418 (1986).

17 August 1992; accepted 13 November 1992

Late Cenozoic Uplift of Denali and Its Relation to Relative Plate Motion and Fault Morphology

Paul G. Fitzgerald, Edmund Stump, Thomas F. Redfield

Apatite fission-track analysis of samples that cover a 4-kilometer vertical section from the western flank of Denali (Mount McKinley), North America's highest mountain, suggests that the mountain massif was formed by rapid uplift (>1 kilometer per million years) beginning ~6 million years ago (Ma). Uplift was a result of the morphology of the Denali fault and a change in motion of the Pacific plate with respect to North America at ~5 Ma, which created opposing tangential vectors of relative movement along the fault and forced the intervening crustal blocks upward.

Terrane theory provides a framework within which the development of the western Cordillera of North America is perhaps best understood (*1*). Quantification of the geometric interactions between the North American, Farallon, Kula, and Pacific plates can help constrain the geologic history of Cordilleran terranes and the kinematics of their boundaries (*2*). Together, plate motion models and geochronologic studies can place significant constraints on geologic interpretations.

During the late Mesozoic and early Tertiary, the accretion of exotic terranes reshaped the margin of western North America (*1, 3, 4*). In southern Alaska, subsequent thrusting and strike-slip faulting dissected these terranes. Boundaries between terranes and dissected fragments are now complex deep-seated ductile shear zones that may show evidence for recurrent movement (*4, 5*). The Denali fault system (DFS), a major crustal break, has experienced both postaccretionary dextral shear and vertical high-angle reverse movements (Fig. 1) (*5–7*). The still-active McKinley strand of the DFS truncates the Hines Creek fault, along which little major strike-slip movement has occurred since 95 Ma. Some dip-slip and local strike-slip motion may have occurred in the Paleocene and in Recent times along the Hines Creek strand (*8*). Estimates of dextral offset along the McKinley fault strand since Oligocene time vary from <10 to 38 km (*6, 9*). Elsewhere along the DFS, estimates of post-Mesozoic dextral offset vary from ~400 to ~200 km (*7, 8*). Alternatively, apparent horizontal displacement of terranes along the DFS may be a result of thousands of meters of vertical offset combined with only a few kilometers of dextral movement (*4, 6*). In this report we suggest a cause of uplift for the Denali area by integrating apatite fission-track data, relative plate motions, and regional geological and geophysical constraints.

In Denali National Park south of the McKinley strand, granite plutons intrude undifferentiated Jurassic-Cretaceous flysch. Plutonic rocks of south-central Alaska were emplaced in the early and middle Jurassic (176 to 154 Ma), the late Cretaceous and early Tertiary (83 to 56 Ma), and the middle Tertiary (38 to 28 Ma) (*10*). Most of the plutons in the Denali region (the McKinley sequence) are undeformed and of late Cretaceous to early Tertiary age, although some middle Tertiary plutons are also present. By the late Mesozoic, the terranes of south-central Alaska were assembled, although not necessarily in their present location. South of the McKinley strand, the granitic massifs of Denali (6194 m), Mount Foraker (5183 m), and Mount Hunter (4441 m) dominate the Alaska Range. Differential erosion has undoubtedly accentuated these peaks; the rest of the range is composed largely of less competent metasedimentary rocks. Nearby, other largely granitic massifs along the DFS, such as the Kichatna Mountains and the Mount Deborah region, have lower elevations and less relief.

Apatite fission-track thermochronology provides information on the timing, rate, and amount of uplift and exhumation of mountain belts (*11*). The temperature zone of track retention depends on cooling rate and chemical composition. Apatites from the McKinley plutons have compositions similar to that of Durango apatite, an age standard in which tracks are effectively retained at temperatures less than ~110°C for cooling rates of 0.1° to 10°C per million years over geologic time (*12*). In stable thermal and tectonic situations, distinctive apatite age-temperature profiles develop. Tracks effectively anneal instantaneously at temperatures >110°C, but slowly at tem-

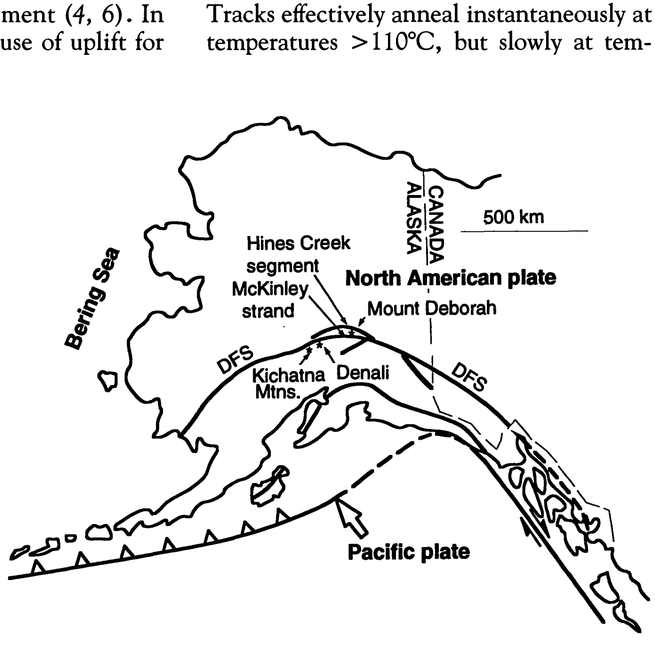

Fig. 1. Location map of Alaska showing the Denali fault system and other major tectonic features. [Modified from (*7*)]

Department of Geology, Arizona State University, Tempe, AZ 85287.